Analysis of Micro-Vacuum Arc Thrusters for Earth-Orbiting and Lunar Missions

IEPC-2011-031

Therese R. Suaris [1]
George Washington University, Washington, D.C.20052, USA
NASA Goddard Space Flight Center, Greenbelt, MD 20771, USA

Michael Keidar[2]
George Washington University, Washington, D.C.20052, USA

Abstract: **The Micro-Vacuum Arc Thruster (VAT) is a propulsion system that uses an arc to evaporate solid cathode material. The propulsion system is compatible for nano-satellite applications due to its low operating voltage, low mass, and its simplicity to be integrated into the spacecraft operating system. The VAT experimental performance values were used to baseline the numerical thruster model for the space mission operations scenario. The simulation results were used analyze the performance parameters that are required for maneuvers and interplanetary trajectories. It is shown that the propulsion system can be used as a low-cost, high performance solution for future CubeSat science and exploration missions that are looking to go beyond the boundaries of the Earth.**

I.   Introduction

Preliminary design analysis of space exploration missions are continuing to be interested in dynamic high performance and low cost solutions that maximizes the scientific, discovery, and engineering goals. The development of new technologies are now allowing for smaller spacecraft designs that are opening the doors to explorers to use these smaller-scale, low-budget orbiting assets to extend the discovery efforts to new frontiers. The use of new propulsion technologies with unique orbit designs will allow for this growth in exploration efforts to continue in a direction that allows for new engineering and technology developments as well.

Over the recent years there has been a great deal of interest in the development of the technology behind the vacuum arc thruster. While interest in using vacuum arc driven electric thrusters as part of spacecraft propulsion systems began in the late 1960s and early 1970s, the engineering behind this technology has grown considerably over the recent years due to its low mass and scalability as a micro-propulsion subsystem. However, the trajectory analysis with these propulsion systems have used non-standardized sets of mission modelling tools that cannot be integrated with and are not compatible with standardized tools that are used for detailed and advanced systems engineering analysis. In addition, previous studies have not considered a wide range of applications for the thruster to support mission around different central bodies.

The innovative approach presented here uses the analytical and experimental results as a baseline to develop a numerical model that is used simulate several case studies of mission scenarios and orbital maneuvers. The overall goal of the study with its many parts was to analyze the application of these engineering developments to actual exploration missions to satisfy requirements on low-maintainability, low-mass, high performance, and more importantly low costs. The results on the low-thrust propulsion system are not point solutions that are tied to a specific set of constraints and mission requirements, but rather the family of results with the models that were

---

[1] Aerospace Systems Engineer, NASA Goddard Space Flight Center, therese.r.suaris@nasa.gov
[2] Professor of Engineering, Department of Mechanical and Aerospace Engineering, keidar@gwu.edu

developed can be used for preliminary mission designs for a wide range space applications as shown by each of the case studies. The analysis enhances the capability of a standardized mission modeling toolset that ensures the applicability of these models and results for the overall systems engineering analysis.

II.   Background Details

A. Technology Development

Interest in using vacuum arc driven electric thrusters as part of spacecraft propulsion systems began in the late 1960s and early 1970s. Interest has focused on reviewing the interaction between vacuum arcs and an applied magnetic field [1]. The high velocity and highly directional nature of the plasma plume expanding from the cathode drew a lot of interest for using vacuum arcs in electric propulsion systems. Previous research efforts have measured the cathodic erosion of Copper, Chromium, and Cadmium for a range of DC currents [2]. The Micro-Vacuum Arc Thruster (VAT) [3, 4] is a propulsion system that uses an arc to evaporate solid cathode material. As shown in Figure 1, the VAT includes an insulator that separates the tubular solid anode and the cathode that enclose the magnetically enhanced vacuum arc [5]. The

Figure 1. Schematic of the Magnetically Enhanced Vacuum Arc Thruster [3].

operating concept for the thruster uses the natural expansion of arc plasma jet in the vacuum that creates a self-consistent ambipolar electric field in the expanded plasma where ions are accelerated in the plasma jet. The magnetic field that is applied to enhance the VAT transforms the radial cathode jet flow into an axial flow. The arc spot occurs at the edge between the metallic cathode and the ceramic spacer ring and multiple spots exit depending on the current and the cathode material that is used. In addition, the use of the magnetic field leads to the cathode spot motion in the azimuth direction that results in uniform cathode erosion.

Any electrically conductive material can be used to produce these vacuum arcs. A range of these materials have been studied over the years to determine their applicability to be used as part of a VAT electric propulsion system. Several electric propulsion systems have used capacitive energy storage [6]. It has been demonstrated that the vacuum arc thrusters operate in a pulsating manner and in addition it has been shown that the overall thrust efficiency of the engine depends on the amplitude and duration of the current pulses along with material used for the electrode. The high erosion rate of metals with low thermal conductivity and low melting points makes the material dependence and selection an important aspect of ensuring high thrust efficiencies for the thruster [3]. In addition, the scalability of the vacuum arc thruster makes it a great candidate for a micro-propulsion subsystem [7].

The VAT has several interesting characteristics that have made it appealing for space applications. These include the use of a low voltage and a solid fuel for operations, and the ease in controllability with the adjustment of the arc current and repetition rate. While the VAT has a high exit velocity, there is a range of options for cathode material selection that allows for customizing high thrust efficiency during any operational scenario. Interest in electric propulsion has increased over the years due to its economic savings for space exploration missions and its promise to revolutionize science missions. Recent NASA sponsored activities at NASA centers and industry/academia on electric propulsion have focused on developing these technologies to enable new mission objectives and to expand these developments to industry and commercial space exploration efforts [8]. Research efforts include Hall thruster technology, pulsed plasma thruster technology, gridded ion thruster technology, high-power electric propulsion technology (for example, Magnetoplasmadynamic thrusters and pulsed inductive thrusters), and supporting systems technology needed for implementation of advanced concepts. In addition, studies have focused on the performance of clusters of Hall and ion thrusters. Science and mission requirements that drive mission analysis have guided these technology programs and demonstrate new capabilities to mission designers. In addition, NASA is exploring options for high-power thruster systems that use nuclear power including both reactor and radioisotope power sources. Coordinating these research efforts with those conducted by the Department of Defense and other national agencies allows for the effective use of available resources. Key examples of NASA satellites with electric propulsion includes the Earth Observing-1 (EO-1) spacecraft that has demonstrated the successful operation of the pulsed plasma thruster and the DAWN asteroid science mission that uses NSTAR Ion thrusters with Xenon as its propellant.

B. Performance Characterization of the Thruster

The magnetically enhanced vacuum arc thruster has shown several advantages for space applications including maneuvering and control of nanosatellites [5]. In addition, it has been shown that there is cathode spot motion in the azimuth direction because of the magnetic field and this in turn causes uniform erosion of the cathode material. Additional research work has focused on modeling the thruster to better understand the effect of the external magnetic field on the thruster operations. Measurements of the ion velocity that is related to the specific impulse were made as a function of the applied magnetic field, the uniform discharge that effects the lifetime of the thruster, and plume contamination due to plasma plume distribution. The results showed that as the magnetic field is increased, there is an increase in the ion drift velocity. Additional measurements were done using Langmuir probes to measure the rotation of the cathode spot due to the applied magnetic field and special concentric circular probes to measure ion current distributions outside the thruster channel.

C. Low-Thrust Trajectory Analysis

Several low-thrust trajectory optimization tools have been developed in the recent years [9, 10]. To perform analysis for a wide trade space and to incorporate advanced mission designs, the toolset includes both low-medium and high fidelity tools. The performance of these tools has been tested and compared using a set of reference trajectories. While for certain trajectories low, medium, and high fidelity tools provide approximately close solutions, the high fidelity allows for complex mission modeling more often than providing high accuracy [11, 12]. However, low-fidelity tools have faster computation times and can perform faster trade study analysis to explore specific mission requirements and objective. The low-thrust trajectory optimization algorithm was developed for preliminary design analysis. The methodology discretized the trajectory into segments that is optimized by a non-linear numerical integration method. While the tool provides robust convergence and has several low-thrust propulsion models, it is limited to simplified, preliminary mission analysis that is not compatible with standardized models and analysis tools. While having a large set of tools provide options on what tools one can be used for a specific study, it can also cause confusion for overall system and mission designers when different analysts might use different tool to come to different solutions for the same problem. In addition, these result in non-standardized sets of tools that used non-standardized asset models, can then be used across groups that might not be compatible with standardized tools for detailed and advanced systems engineering analysis. Using standardized sets of tools allow mission designers to rapidly analyze and compare results and to integrate other trajectory analysis with other subsystems including communications, coverage, mechanical, and thermal systems.

Several unique methodologies have also been used for low-thrust trajectory analysis The Tisserand graphical technique is used for low-thrust gravity-assist trajectory design that is only applicable for preliminary mission design phases [13] as it is a simplified process that doesn't take into account various other propulsion and mission parameters that affects the performance of the spacecraft trajectory. For mission design analysis, selecting a specific electric propulsion system, launch vehicle, and flight time have significant impacts on the performance and robustness of the mission as well as the overall cost of the mission [14, 15]. While a simplified analysis can provide some insight on designing cost efficient systems, using the mass alone as a constraint is insufficient to determine a minimum cost solution without taking into account all of the key mission and performance parameters and all of the mission requirements.

Previous analysis has also been presented on optimizing low-thrust transfers using an initial guess-free methodology [16]. Additional work has focused on mission analysis for high-power mission analysis to determine propulsive requirements [17, 18]. The method uses only a few configuration parameters to reduce the optimization time that limits the applicability of the methodology to early mission designs and doesn't take into account additional parameters that allows for transfer orbit analysis with multiple bodies under various perturbations. In addition, previous research work have performed preliminary low-thrust trajectory designs for the Earth-moon three-body problem for variable specific impulses and fixed power [19]. While the results from the analysis can be used for an initial proof-of-concept for an Earth-moon libration point mission, the analytical mission analysis doesn't take into account the non-linear properties of the problem including external perturbations and a complete engine model on a standardized set of tool including all mission and performance parameters.

III. Modeling and Simulation

A. Simulation Environment

Satellite Toolkit (STK) is a modeling and simulation program that is used to accurately define and model space assets in a real-time or simulated environment [20]. The properties of assets can be modified in a dynamic environment for a specified time duration using different models, propagators, and external inputs. These dynamic models can be used to model the interaction between multiple assets and can be further extended for access, coverage, communications, and other analysis. In addition, constraints can be defined within the scenario to account for real-life environmental losses and other conditions that are not accounted for in equations derived for ideal conditions. The analysis tool was used to model each of the scenarios that are described in the following chapters around the Earth, Moon, and libration points. The thruster was modeled as an engine model as described below for the single thruster configuration and a thruster set for the stacked configuration with the use of experimental data as the baseline. In addition, STK/Astrogator was used to model the complex trajectory design and maneuvers around the central bodies and libration points. The propagators used for the analysis numerically integrate the differential equations of motions to generate the satellite's ephemeris. The force models for the Moon HPOP propagator considers the effects of the gravitational field (LP165P model to degree and order of 165), third-body effects (Earth, Sun, and Jupiter), and solar radiation pressure (spherical SRP model). A 7th order Runge-Kutta-Fehlberg integrator with 8th order error control is used as the integrator in the propagator. In addition, The JPL DE421 ephemeris files are included to consider the eccentricity effects of the Earth and Lunar orbits on the spacecraft.

B. Dynamic Modeling and Simulation

As part of this research effort, the simulation environment was used to build a numerical model of the thruster at different configurations to conduct an extensive study on its application to propel space missions and maneuvers around the Earth and beyond. The innovative approach uses the analytical and experimental results as a baseline to develop a numerical model that is used to simulate several case studies of mission scenarios and orbital maneuvers. In contrast to previous analytical studies, the numerical study presented in this analysis takes into account detailed and actual perturbations for space mission maneuvers that is not a point solution but the model can be used to examine a range of applications as shown by the different case studies that were considered as part of this study. The analysis enhances the capability of a standardized mission modeling toolset that ensures the applicability of the built models and results for the overall systems engineering analysis for preliminary mission design applications.

Unlike previous research efforts, several case studies were modeled and simulation using the numerical models as part of this study to examine the applicability of the vacuum arc thruster for space mission trajectories and maneuvers around various central bodies. The Earth based case studies that were examined includes station-keeping maneuvers, apogee and perigee raises, and transfer orbits including low-altitude transfers and geostationary transfers, as shown in the example shown in Figure 2. Similarly, the lunar case studies examined the transfer orbits with apogee and perigee raises and station-keeping requirements. In addition, the case studies extended the analysis to examine the performance parameters to support Earth-Moon libration point orbits including transfer orbits and station-keeping maneuvers. Each of the scenarios that were modeled with the input data was used to calculate the performance parameters for the thruster operations including the number of pulses, fuel mass requirements assuming a cathode consumption of 4 x 10^6 pulses per gram of cathode mass, and the total operating time estimates for different pulse operating frequencies. The scenario was modeled for a single VAT engine model and thruster set at different stacked configurations. An example of the stacked array is shown in Figure 3, where the single engine is presented along with the four engine stacked thruster set configuration.

The thruster set scenarios were modeled with single engines firing in the different coordinate directions and multiple engines in a stacked array starting with two engines operating in the different directions. The 12 engine stacked array configuration was designed with four engine models in a stacked configuration firing in the three coordinate directions. Note that the total operating time presented in the results section for the thruster set configurations are for all the thrusters. Therefore, if the thrusters are operating simultaneously the overall operating time is less than that for a single engine. research effort discussed in this paper is focused on verifying and validating the development of the thrusters and more importantly showing its applicability to support space missions to perform propulsion functions. The experimental performance impulse bit values are used to baseline the numerical model that is written as a plug-in script for the propulsion system to perform maneuvers for the simulated scenarios. Several propulsion functions were modelled for various space operating scenarios including Earth-orbiting and Lunar missions as shown in Figures 4 and 5. An example of an Earth-Lunar target profile is shown in Figure 4 that uses differential corrector methods to target the Lunar orbit from an Earth launch. Varying each of the profile

propulsion functions and target profiles provided a range of data on the performance of the thrusters while Figure 5 provides another mission operating scenario around the Earth for an apogee raise to a 300 km orbit.
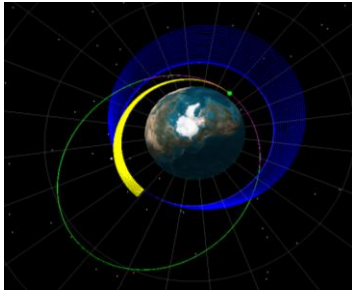
Figure 2. Example Earth-based Mission Scenario.
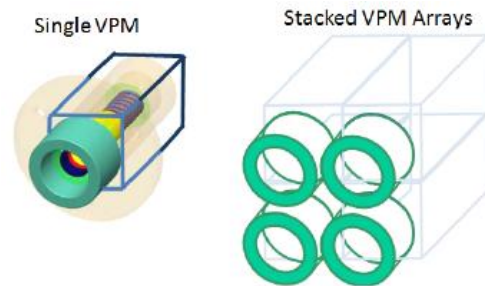
Figure 3. VPM Configuration Examples [5].
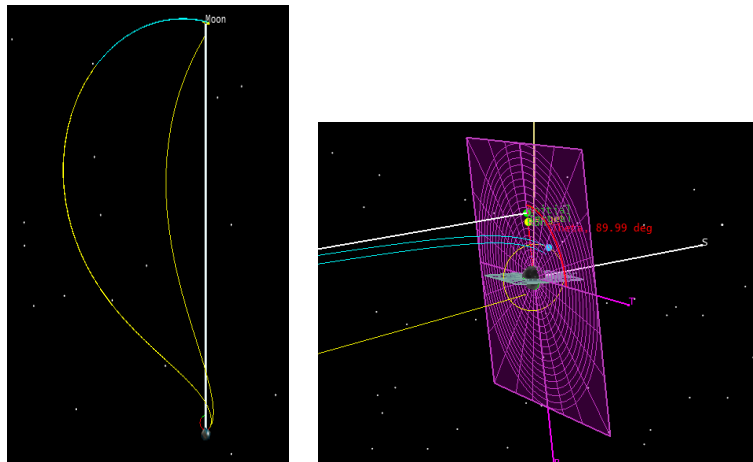
Figure 4. Earth-Lunar targeting profile scenario targets a trajectory from Earth launch to a desired Lunar orbit.
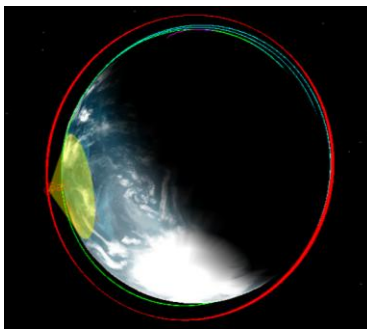
Figure 5. An example of an Earth-orbiting mission profile scenario.

IV.   Results

Several case studies were examined as part of this study to calculate performance parameter requirements for the thruster application in space mission scenarions. The low-Earth apogee raise scenario was modeled for a range of target altitudes including 300 km, 500 km, 750 km, and 1000 km. Similarly, the low-Earth perigee raise scenario was modeled for a range of target altitudes including 300 km, 500 km, 750 km, and 1000 km. In addition, it modeled a range of target eccentricities of 0, 0.05, and 0.1 and a range of target inclinations 50, 60, 70, 80, and 90 degrees. The Earth-based two-maneuver scenario was modeled for a range of target altitudes including 300 km, 350 km, 500 km, 1000 km, 1500 km, and 2000 km and the Earth-based de-orbiting scenario was modeled for a range of target altitudes including 100 km, 300 km, 500 km, and 1000 km. The geosynchronous orbit transfer and maintenance scenario modeled an apogee raise to a geostationary transfer orbit and the transfer to a geostationary orbit. The scenario also modeled the Hohmann transfer with the apogee raise and circularization of the orbit as it targeted the eccentricity. The station-keeping segments modeled the drift maneuver for the East-West station-keeping and the adjustment of the right ascension of the ascending node for North-South station-keeping. The transfer scenario from the elliptic orbit to the geosynchronous orbit was modeled from an initial elliptic orbit with a periapsis altitude at 9000 km, eccentricity at 0.5, inclination at 28.5 degrees, and right ascension of the ascending node at 45 degrees. The target apogee was at 42165 km and target perigee with eccentricity equal to 0 and inclination equal to 0 degrees. The lunar target scenario was modeled both a 50 km and 500 km target altitudes with a 90 degrees inclination. The lunar apogee and perigee raise scenario was modeled for a low altitude 10 km lunar orbit. In addition, the libration point target scenario was modeled to target the L1 and L2 libration points and station keeping.

All the scenarios were modeled for a single VAT engine model and thruster set with four engine models in a stacked configuration firing in the three coordinate directions. The impulse bit is calculated using experimental results for a given thrust duration of 250 micro-seconds and a range of specific impulse values of 1000 sec, 2000 sec, and 3000 sec. The results were calculated for range of thrust values that was derived from the impulse bit and pulse thrust duration data. In addition, the analysis was extended to a range of 1 kg, 2 kg, 3 kg, and 5 kg dry mass values. The scenarios that were modeled with the input data is used to calculate the performance parameters for the thruster operations including the number of pulses, fuel mass requirements assuming a cathode consumption of 4 x 10^6 pulses per gram of cathode mass, and the total operating time estimates for different pulse operating frequencies.

The example summary tables shown below provide the performance data for the single engine configuration for the increased impulse bit for increased performance where the impulse bit is equal to 1.5 x 10^{-5} N*s, thrust duration equal to 0.00025 sec, thrust equal to 6 x 10^{-2} N, and specific impulse equal to 1000 sec. For the 300 km Earth-based apogee raise at a single engine configuration, using the current experimental model input configuration parameters resulted in performance parameter requirements equal to a fuel mass of 18.3 grams and a total operating time of 0.57 months for a 50 Hz pulse repetition rate while for the increased configuration the fuel mass is reduced to 0.274 grams and the operating time can be reduced to as much as 0.008 months as shown in Table 1. For the 300 km Earth-based perigee raise at a single engine configuration for a target eccentricity of 0 and inclination of 50 degrees, using the current experimental model input configuration parameters resulted in performance parameter requirements equal to a fuel mass of 13.4 grams and a total operating time of 0.41 months for a 50 Hz pulse repetition rate while for the increased configuration the fuel mass is reduced to 0.2 grams and the operating time can be reduced to as much as 0.01 months as shown in Table 2. For the 300 km to 350 km two-maneuver transfer at a single engine configuration, using the current experimental model input configuration parameters resulted in performance parameter requirements equal to a fuel mass of 16.99 grams and a total operating time of 0.52 months for a 50 Hz pulse repetition rate while for the increased configuration the fuel mass is reduced to 0.26 grams and the operating time can be reduced to as much as 0.01 months as shown in Table 3. For the 300 km to 100 km de-orbit scenario at a single engine configuration, using the current experimental model input configuration parameters resulted in performance parameter requirements equal to a fuel mass of 1314.99 grams and a total operating time of 40.60 months for a 50 Hz pulse repetition rate while for the increased configuration the fuel mass is reduced to 19.73 grams and the operating time can be reduced to as much as 0.61 months as shown in Table 4. For the geosynchronous transfer scenario at a single engine configuration, using the current experimental model input configuration parameters resulted in performance parameter requirements equal to a fuel mass of 1847.73 grams and a total operating time of 57 months for a 50 Hz pulse repetition rate while for the increased configuration the fuel mass is reduced to 27.72 grams and the operating time can be reduced to as much as 0.86 months as shown in Table 5. For the elliptic to geosynchronous transfer scenario at a single engine configuration, using the current experimental model input configuration parameters resulted in performance parameter requirements equal to a fuel mass of 429.77 grams and a total operating time of 13.3 months for a 50 Hz pulse repetition rate while for the

increased configuration the fuel mass is reduced to 6.45 grams and the operating time can be reduced to as much as 0.2 months as shown in Table 6.

For the lunar target scenario at a thruster set configuration, using the current experimental model input configuration parameters resulted in performance parameter requirements equal to a fuel mass of 383.27 grams and a total operating time of 143 months for a 50 Hz pulse repetition rate while for the increased configuration the fuel mass is reduced to 5.75 grams and the total operating time can be reduced to as much as 2.13 months as shown in Table 7. Note that this is the total operating time for all the thrusters. Therefore, if the thrusters are operating simultaneously the overall operating time will be less than that for a single engine. For the lunar apogee and perigee raise scenario at a single engine configuration, using the current experimental model input configuration parameters resulted in performance parameter requirements equal to a fuel mass of 9.63 grams and a total operating time of 0.3 months for a 50 Hz pulse repetition rate while for the increased configuration the fuel mass is reduced to 0.14 grams and the total operating time can be reduced to as much as 0.004 months as shown in Table 8. For the L1 libration point target scenario at a single engine configuration, using the current experimental model input configuration parameters resulted in performance parameter requirements equal to a fuel mass of 697.21 grams and a total operating time of 21.4 months for a 50 Hz pulse repetition rate while for the increased configuration the fuel mass is reduced to 10.41 grams and the total operating time can be reduced to as much as 0.32 months as shown in Table 9.

Table 1. Summary increased performance parameters for the Earth-based apogee raise for the single engine configuration.

		Number of Pulses	Fuel Mass Consumed (grams)	Total Operating Time (months) - 1 Hz Repetition Rate	Total Operating Time (months) - 50 Hz Repetition Rate
300 km	1 kg	1.10E+06	0.274	0.424	0.008
500 km	1 kg	4.78E+06	1.195	1.840	0.037
750 km	1 kg	9.24E+06	2.311	3.570	0.071
1000 km	1 kg	1.35E+07	3.374	5.210	0.104

Table 2. Summary increased performance parameters for the perigee raise for the single engine configuration.

				Number of Pulses	Fuel Mass Consumed (grams)	Total Operating Time (months) - 1 Hz Repetition Rate	Total Operating Time (months) - 50 Hz Repetition Rate
300 km	1 kg	e=0	i=50 deg	8.04E+05	0.20	0.31	0.01
			i=60 deg	8.39E+07	20.97	32.40	0.65
			i=70 deg	1.57E+08	39.17	60.40	1.21
			i=80 deg	2.19E+08	54.81	84.60	1.69
			i=90 deg	2.73E+08	68.19	105.00	2.10
500 km	1 kg	e=0	i=50 deg	4.37E+06	1.09	1.68	0.03
			i=60 deg	8.23E+07	20.59	31.80	0.64
			i=70 deg	1.54E+08	38.47	59.40	1.19
			i=80 deg	2.15E+08	53.85	83.10	1.66
			i=90 deg	2.69E+08	67.13	104.00	2.07
1000 km	1 kg	e=0	i=50 deg	1.29E+07	3.21	4.96	0.10
			i=60 deg	7.97E+07	19.93	30.80	0.62
			i=70 deg	1.48E+08	37.07	57.20	1.14
			i=80 deg	2.08E+08	52.00	80.30	1.61
			i=90 deg	2.60E+08	64.90	100.00	2.00
1000 km	1 kg	e=0.05	i=50 deg	6.55E+05	0.16	0.25	0.01
			i=60 deg	8.29E+07	20.73	32.00	0.64
			i=70 deg	1.51E+08	37.73	58.20	1.16
			i=80 deg	2.11E+08	52.68	81.30	1.63
			i=90 deg	2.62E+08	65.61	101.00	2.02
1000 km	1 kg	e=0.1	i=50 deg	1.20E+07	3.01	4.65	0.09
			i=60 deg	8.72E+07	21.80	33.60	0.67
			i=70 deg	1.54E+08	38.51	59.40	1.19
			i=80 deg	2.14E+08	53.42	82.40	1.65
			i=90 deg	2.65E+08	66.35	102.00	2.05

Table 3. Summary increased performance parameters for the two-maneuver transfer for the single engine configuration.

		Number of Pulses	Fuel Mass Consumed (grams)	Total Operating Time (months) - 1 Hz Repetition Rate	Total Operating Time (months) - 50 Hz Repetition Rate
300 km - 350 km	1 kg	1.02E+06	0.26	0.39	0.01
	2 kg	2.04E+06	0.51	0.79	0.02
300 km - 500 km	1 kg	3.83E+06	0.96	1.48	0.03
	2 kg	7.67E+06	1.92	2.96	0.06
500 km - 1000 km	1 kg	8.82E+06	2.204	3.40	0.07
	2 kg	1.76E+07	4.408	6.80	0.14
1000 km - 1500 km	1 kg	7.96E+06	1.99	3.07	0.06
	2 kg	1.59E+07	3.98	6.14	0.12
1500 km - 2000 km	1 kg	7.24E+06	1.81	2.79	0.06
	2 kg	1.45E+07	3.62	5.58	0.11

Table 4. Summary increased performance parameters for the de-orbit transfer for the single engine configuration.

		Number of Pulses	Fuel Mass Consumed (grams)	Total Operating Time (months) - 1 Hz Repetition Rate	Total Operating Time (months) - 50 Hz Repetition Rate
300 km - 100 km	1 kg	7.89E+07	19.73	30.40	0.61
	2 kg	1.58E+08	39.45	60.90	1.22
1000 km - 500 km	1 kg	8.42E+07	21.06	32.50	0.65
	2 kg	1.68E+08	42.11	65.00	1.30

Table 5. Summary increased performance parameters for the geosynchronous transfer and station-keeping for the single engine configuration.

		Number of Pulses	Fuel Mass Consumed (grams)	Total Operating Time (months) - 1 Hz Repetition Rate	Total Operating Time (months) - 50 Hz Repetition Rate
Apogee Raise to GTO	1 kg	1.43E+08	35.83	55.30	1.11
	2 kg	2.87E+08	71.65	111.00	2.21
	3 kg	4.30E+08	107.48	166.00	3.32
Prop to GEO	1 kg	1.11E+08	27.72	42.80	0.86
	2 kg	2.22E+08	55.43	85.50	1.71
	3 kg	3.33E+08	83.15	128.00	2.57
Hohmann Transfer Apogee Raise	1 kg	2.99E+05	0.08	0.12	0.002
	2 kg	5.98E+05	0.15	0.23	0.005
	3 kg	8.97E+05	0.22	0.35	0.007
NS Station Keeping - Circularize	1 kg	2.62E+05	0.07	0.10	0.002
	2 kg	5.25E+05	0.13	0.20	0.004
	3 kg	7.87E+05	0.20	0.30	0.006
EW Station Keeping - Drift Maneuver	1 kg	8.00E+03	0.002	0.003	0.00006
	2 kg	1.60E+04	0.004	0.006	0.00012
	3 kg	2.40E+04	0.006	0.009	0.00019
NS Station Keeping -RAAN Adjust	1 kg	1.32E+07	3.30	5.09	0.10
	2 kg	2.64E+07	6.60	10.20	0.20
	3 kg	3.96E+07	9.90	15.30	0.31

Table 6. Summary increased performance parameters for the geostationary transfer and station-keeping for the single engine configuration.

		Number of Pulses	Fuel Mass Consumed (grams)	Total Operating Time (months) - 1 Hz Repetition Rate	Total Operating Time (months) - 50 Hz Repetition Rate
Target Apogee	1 kg	2.58E+07	6.45	9.95	0.20
	2 kg	5.16E+07	12.89	19.90	0.40
	3 kg	7.74E+07	19.34	29.80	0.60
Target Perigee	1 kg	1.05E+08	26.16	40.40	0.81
	2 kg	2.09E+08	52.32	80.70	1.61
	3 kg	3.14E+08	78.48	121.00	2.42

Table 7: Summary increased performance parameters for the lunar target for the thruster set configuration.

		Number of Pulses	Fuel Mass Consumed (grams)	Total Operating Time (months) - 1 Hz Repetition Rate	Total Operating Time (months) - 50 Hz Repetition Rate
Target Low Altitude (< 500 km)	1 kg	2.30E+07	5.75	106.00	2.13
	2 kg	4.60E+07	11.50	213.00	4.26
	3 kg	6.90E+07	17.24	319.00	6.39
Target Perigee	e=0	1 kg	9.00E+07	22.49	34.70	0.69
	e=0.05		8.58E+07	21.46	33.10	0.66
Target Perigee 500 km	e=0	1 kg	8.44E+07	21.09	32.50	0.65
	e=0.05		8.06E+07	20.16	31.10	0.62
	e=0.1		7.69E+07	19.23	29.70	0.59
	e=0.2		6.98E+07	17.46	26.90	0.54
	e=0.3		6.30E+07	15.74	24.30	0.49
	e=0.4		5.63E+07	14.08	21.70	0.43

Table 8. Summary increased performance parameters for lunar apogee and perigee raise for the single engine configuration.

		Number of Pulses	Fuel Mass Consumed (grams)	Total Operating Time (months) - 1 Hz Repetition Rate	Total Operating Time (months) - 50 Hz Repetition Rate
Target Perigee	1 kg	5.78E+05	0.14	0.22	0.004
	2 kg	1.16E+06	0.29	0.45	0.009
	3 kg	1.73E+06	0.43	0.67	0.013
Target Apogee	1 kg	6.90E+05	0.17	0.27	0.005
	2 kg	1.38E+06	0.35	0.53	0.011
	3 kg	2.07E+06	0.52	0.80	0.016

Table 9. Summary increased performance parameters for the libration target for the single engine configuration.

		Number of Pulses	Fuel Mass Consumed (grams)	Total Operating Time (months) - 1 Hz Repetition Rate	Total Operating Time (months) - 50 Hz Repetition Rate
Target L1	1 kg	4.17E+07	10.41	16.10	0.32
	2 kg	8.33E+07	20.83	32.10	0.64
L1 - 1 Rev	1 kg	3.08E+04	0.008	0.012	0.0002
	2 kg	6.15E+04	0.015	0.024	0.0005
L1 - 2 Rev	1 kg	2.16E+03	0.001	0.0008	0.00002
	2 kg	4.32E+03	0.001	0.0017	0.00003
Target L2	1 kg	5.99E+07	14.98	23.10	0.46
	2 kg	1.20E+08	29.96	46.20	0.93
L2 - 1 Rev	1 kg	1.80E+03	0.0005	0.0007	0.000014
	2 kg	3.60E+03	0.0009	0.0014	0.000028
L2 - 2 Rev	1 kg	1.82E+03	0.0005	0.0007	0.000014
	2 kg	3.63E+03	0.0009	0.0014	0.000028
L2 - 3 Rev	1 kg	4.77E+03	0.001	0.0018	0.000037
	2 kg	9.53E+03	0.002	0.0037	0.000074
L2 - 4 Rev	1 kg	4.39E+03	0.001	0.0017	0.000034
	2 kg	8.78E+03	0.002	0.0034	0.000068

V.   Discussion

The summary results data and tables were presented in two sections where the first noted the performance parameters for the current average experiment conditions while the other presents the performance parameters when the current conditions are improved to a higher impulse bit and thrust value. The results shown under the current average conditions show that the engine is best suited for station-keeping maneuvers rather for transfer orbit maneuvering due to the large fuel mass requirements and long operating time requirements associated with these large delta-V maneuvers. The operating time improves as the frequency of repetition rate of the pulses is increased from 1 Hz to 50 Hz. In addition, the individual operating time of the engine can be reduced when multiple engines are used in a stacked configuration operating simultaneously in different directions. However, the tables on the increased performance conditions show that as the thrust value is increased with higher impulse bit values then the engine and thruster set can be used for many more space mission applications including station-keeping and transfer orbits around the Earth and other central bodies. In addition, there are differences between the operation of the single engine and thruster set configuration because of changes in the attitude and orbital control of the maneuvers and transfer scenarios and differences in the propagation and perturbation models used for the modeling and simulations.

A detailed comparative study was done on the mission models and simulations to consider the differences in the performance parameters as the values of the parameters were increased and decreased and when compared to current and developing spacecraft propulsion systems. Increasing the thrust with the impulse bit reduces the operating time and the fuel mass requirements as shown in the summary tables shown in the previous results section. While the operating time is reduced with some of the other comparative propulsion system the requirement fuel mass is increased to very large values with increased delta-v requirements making these systems unable to support smaller CubeSat type missions. While the operating time of the current average pulsed operating system has a higher operation time, improving the parameter values as shown in the tables increases the applicability of the thruster to support many mission requirements with smaller fuel mass requirements. In addition, the scalability of the single engine or the thruster set makes the system more favorable for these missions and the pulsed system provides the mission more control to interactively modify the performance parameters which is not always possible with some of the fixed conditions associated with current propulsion systems. It is also important to note that the space mission scenarios were modeled in a standardized toolset that allows the results to be incorporated to systems engineering applications. In addition, the numerical engine and thruster models are based on experimental data to verify current

performance values and to determine improvements to the performance parameters for future applications. Each of the scenarios can be customized to model specific mission requirements as the overall model and process is not constrained to any specific set of conditions. The results from the range of case studies considered in this work is therefore applicable for a wide range of mission applications and the can be further modified for specific applications.

VI.   Conclusion

The simulations provided knowledge and performance outputs for each of the propulsion functions so that requirements and constraints can be generated to determine operability and applicability to support the next generation science and exploration missions. The performance results of the vacuum arc thruster provided insight into the applicability of these technologies for CubeSat mission designs. The results presented as part of this study can be used to build preliminary mission analysis to satisfy high-performance and low cost mission requirements. The mission analysis also provided insight into a low-maintenance and low-mass system. The results shown under the current average conditions show that the engine is best suited for station-keeping maneuvers rather for transfer orbit maneuvering due to the large fuel mass requirements and long operating time requirements associated with these large delta-V maneuvers. The operating time improves as the frequency of repetition rate of the pulses is increased from 1 Hz to 50 Hz. In addition, the individual operating time of the engine can be reduced when multiple engines are used in a stacked configuration operating simultaneously in different directions. However, the result tables on the increased performance conditions show that as the thrust value is increased with higher impulse bit values then the engine and thruster set can be used for many more space mission applications including station-keeping and transfer orbits around the Earth and other central bodies. While the operating time is reduced with some of the other comparative propulsion system the requirement fuel mass is increased to very large values with increased delta-v requirements making these systems unable to support smaller CubeSat type missions. In addition, the scalability of the single vacuum arc engine or the thruster set makes the system more favorable for these missions and the pulsed system provides the mission more control to interactively modify the performance parameters which is not always possible with some of the fixed conditions associated with current propulsion systems. The innovative approach to mission analysis presented here enhances the capability of a standardized mission modeling toolset that ensures the applicability of these models and results for the overall systems engineering analysis. In addition, the numerical engine and thruster models are based on experimental data to verify current performance values and to determine improvements to the performance parameters for future applications. Therefore, the results from the range of case studies considered in this work is applicable for a wide range of mission applications and the can be further modified for specific space exploration mission applications. Also, the results presented in this paper are not point solutions that are tied to a specific set of constraints and mission requirements but rather can be used for wide range space mission applications. In addition, the results provide recommendations into the thrust requirements and other performance parameters that will be needed to build advanced experimental models.

References

1. Gorman, J.G., Kimblin, C.W., Voshall, R.E., Wien, R.E., and Slade, P.G., "The Interaction of Vacuum Arcs with Magnetic Fields and Applications," *IEEE Transactions on Power Apparatus and Systems*, Vol. PAS-102, No. 2, February, 1983.
2. Rondeel, W.G.J., "Cathodic Erosion in the Vacuum Arc," *J. Phys. D: Appl. Phys.,* Vol. 6, 1973.
3. Keidar, M., Schein, J., Wilson, K., Gerhan, A, Au, M., Tang, B., Idzkowski, L., Krishnan, M., and Beilis, I.I., "Magnetically Enhanced Vacuum Arc Thruster," *Plasma Sources Sci. Technol.*, Vol. 14, pp. 661-669, 2005.
4. Zhuang, T., Shashurin, A., Brieda, L., and Keidar, M., "Development of Micro-Vacuum Arc Thruster with Extended Lifetime," 31st International Electric Propulsion Conference, Ann Arbor, Michigan, September 2009.
5. Zhuang, T., Shashurin, A., Haque, S., and Keidar, M., "Performance Characterization of the micro-Cathode Arc Thruster and Propulsion System for Space Applications," Joint Propulsion Conference and Exhibit, Vol. 46, No. AIAA-2010-7018, 2010.
6. Dethlefsen, R. and Ennis, J., "Capacitors for Pulsed Electric Propulsion," 20th International Electric Propulsion Conference, Garmish-Partenkirchen, Germany, IEPC 88-125, October, 1988.
7. Qi, N., Schein, R., Binder, R., Krishnan, M., Anders, A., and Polk, J., "Compact Vacuum Arc Micro-Thruster for Small Satellite Systems," 37th AIAA/ASME.SAE/ASEE Joint Propulsion Conference, Salt Lake City, Utah, 2001.
8. Dunning, J.W. and Jankovsky, R.S., "NASA's Electric Propulsion Program," 39th AIAA/ASME/SAE/ASEE Joint Propulsion Conference and Exhibit, Huntsville, Alabama, AIAA 2003-4437, July, 2003.

9. Polsgrove, T., Kos, L., Hopkins, R., and Crane, T., "Comparison of Performance Predictions for New Low-Thrust Trajectory Tools," AIAA/AAS Astrodynamics Specialist Conference and Exhibit, Keystone, Colorado, AIAA 2006-6742, August 2006.

10. Kos, L.D., Polsgrove, R., Hopkins, R.C., Thomas, D., and Sims, J.A., "Overview of the Development for a Suite of Low-Thrust Trajectory Analysis Tools," AIAA/AAS Astrodynamics Specialist Conference and Exhibit, Keystone, Colorado, AIAA 2006-6743, August 2006.

11. Sims, J.A., Finlayson, P.A., Rinderle, E.A., Vavrina, M.A., and Kowalkowski, T.D., "Implementation of a Low-Thrust Trajectory Optimization Algorithm for Preliminary Design," AIAA/AAS Astrodynamics Specialist Conference and Exhibit, Keystone, Colorado, AIAA 2006-6746, August 2006.

12. Dankanich, J.W., "Low-Thrust Mission Design and Application," 46th AIAA/ASME/SAE/ASEE Joint Propulsion Conference and Exhibit, Nashville, TN, AIAA 2010-6857, July 2010.

13. Chen, K.J., Kloster, K.W., and Longuski, J.M., "A Graphical Method for Preliminary Design of Low-Thrust Gravity-Assist Trajectories," AIAA/AAS Astrodynamics Specialist Conference and Exhibit, Honolulu, Hawaii, AIAA 2008-6952, August 2008.

14. Landau, D., Kowalkowski, T., Sims, J., Randolph, T., Timmerman, P., Chase, J., and Oh, D., "Electric Propulsion System Selection Process for Interplanetary Missions," AIAA/AAS Astrodynamics Specialist Conference and Exhibit, Honolulu, Hawaii, AIAA 2008-7362, August 2008.

15. Landau, D., Chase, J., Randolph, T., Timmerman, P., and Oh., D., " Electric Propulsion System Selection Process for Interplanetary Missions," *Journal of Spacecraft and Rockets,* Vol. 48, No. 3, May-June 2011.

16. Gil-Fernandez, J. And Gomez-Tierno, M.A., " Practical Method for Optimization of Low-Thrust Transfers," *Journal of Guidance, Control, and Dynamics*, Vol. 33, No. 6, November-December, 2010.

17. White, D., Martinez-Sanchez, M., and Daniel, L., "Mission Analysis for Design of High Power Electric Propulsion Thrusters," 45th AIAA/ASME/SAE/ASEE Joint Propulsion Conference and Exhibit, Denver, Colorado, AIAA 2009-5262, August 2009.

18. Gao, Y., "Low-Thrust Interplanetary Transfers, Including Escape and Capture Trajectories," *Journal of Guidance, Control, and Dynamics*, Vol. 30, No. 6, November-December 2007.

19. Ozimek, M.T. and Howell, K.C., "Low-Thrust Transfers in the Earth-Moon System, Including Applications to Libration Point Orbits," *Journal of Guidance, Control, and Dynamics*, Vol. 33, No. 2, March-April, 2010.

20. Analytical Graphics, Inc. web site at www.stk.com.